



Julolidine fluorescent molecular rotors as vapour sensing probes in polystyrene films



Giulio Martini^a, Elisa Martinelli^{a, b}, Giacomo Ruggeri^{a, b}, Giancarlo Galli^{a, b},
Andrea Pucci^{a, b, *}

^a Dipartimento di Chimica e Chimica Industriale, Università di Pisa, Pisa, Italy

^b INSTM, UdR Pisa, Italy

ARTICLE INFO

Article history:

Received 10 June 2014

Received in revised form

17 July 2014

Accepted 18 July 2014

Available online 8 August 2014

Keywords:

Fluorescent molecular rotors

Julolidine derivatives

Polystyrene films

Volatile organic compounds

Vapour sensing behaviour

Reversible behaviour

ABSTRACT

We introduce a new sensing polymer system for detection of volatile organic compounds (VOCs) based on the optical response of polystyrene (PS) films doped with julolidine fluorescent molecular rotors (FMRs). The julolidine FMRs exhibited viscosity-dependent changes in the fluorescence intensity, that was enhanced when glycerol was added to ethanol solutions and when they were dispersed in PS films. Thus, reduction in medium mobility slowed down internal motions and allowed for a major radiative decay pathway. The FMR/PS films were exposed to several VOCs, and showed a significant decrease in fluorescence emission when exposed to chloroform, whereas a negligible variation in their emission occurred when methanol was utilized. This vapour sensing behaviour was much more evident when a perfluorodecyl chain was linked to the julolidine core being the molecule segregated at the film surface. This responsive behaviour was affected by solvent composition and its reproducible response was easily determined by luminescence experiments.

© 2014 Elsevier Ltd. All rights reserved.

1. Introduction

Luminescent materials have been actively pursued recently, owing to their various promising applications in diverse fields, ranging from solar energy conversion [1], to optoelectronic devices [2] and chromogenic materials [3–6]. Chromogenic systems are capable to respond to various stimuli (e.g. light, heat, mechanical stress and chemical stimuli) through a macroscopic optical output [4,7,8]. The energy of the stimulus is properly transduced into optical variations (i.e., absorption, emission, refractive index) as a function of external interference.

Recently, luminescent materials which display reversible colour changes upon exposure to vapours of volatile organic compounds (VOCs), have also rapidly evolved due to their potential application for chemical vapour detection [9–11]. The detection of VOCs can often occur by the naked eye, thus suggesting such systems as promising tools for environmental monitoring and safety systems at workplaces.

The optical response to vapours is often associated with changes in the weak metal–metal interactions of coordination complexes as a result of analyte vapour sorption [9]. As an alternative, solvatochromic fluorescent organic species are used for the detection of organic vapours, since their wavelength emission depends on the polarity of VOCs [12,13]. In the last years, organic luminophors such as tetraphenylethene derivatives [14–17], have been proposed as compounds with effective vapour sensitivity. They display aggregation induced luminescent properties [10,18] and the vapour uptake caused changes in their intermolecular interactions thus affecting molecular packing and emission [19].

For practical applications, those molecules are fabricated into thin solid films or incorporated in polymer matrices. The success of vapour sensing polymer films is largely due to the ability of volatile compounds to spread rapidly inside the polymer matrix and interact with the sensor molecule giving a fast and reliable response [20,21]. The use of visible-light transparent polymer matrices with good film-forming capacity allows also the preparation of large area devices at ambient conditions by low-cost fabrication techniques.

Fluorescent molecular rotors (FMRs) are fluorescent molecules composed by an electron donor unit in conjugation with an electron acceptor moiety and are reported to undergo non-radiative relaxation from the fluorescent excited state [22–24]. More

* Corresponding author. Dipartimento di Chimica e Chimica Industriale, Università di Pisa, Via Risorgimento 35, 56126 Pisa, Italy. Tel.: +39 050 2219270; fax: +39 050 2219260.

E-mail address: andrea.pucci@unipi.it (A. Pucci).

specifically, in the ground state the FMR is almost planar and highly conjugated as well as its locally excited (LE) state. Nevertheless, solvent relaxation and rapid internal torsional motion occur, thus resulting in a twisted intramolecular charge transfer (TICT) excited state, which rapidly decays in a non-radiative way through internal rotation [22,25–27]. Moreover, non-radiative deactivation of the first excited state is controlled by rapid internal torsional motion, which is substantially restricted in viscous media [28,29] When this internal rotation is hindered, e.g. due to an increase in viscosity or steric constraints, the radiative decay of LE state is favoured, and an increase in quantum yield is obtained [27].

The apparent sensitivity to fluid motion of FMRs like julolidine derivatives is also found to be an indirect effect of a photoisomerization reaction [30].

FMRs have received popularity in the last 5–10 years thanks to their easy applicability as non-mechanical viscosity sensors, tools for protein characterization and local microviscosity imaging [31–34]. Moreover, the high sensitivity towards viscosity changes has reached a precision comparable to commercial mechanical rheometers with shorter measurement time [35].

While the application of julolidine FMRs as viscosity sensors is widespread, their behaviour within polymer matrices is still under debate. A few examples have been reported for the determination of the molecular weight dependence of viscosity in polymer melts [36] and for sensing free volume and plasticity in thermoplastic polymers [37,38].

Herein, we report on the emission properties of different julolidine FMRs dispersed (~0.05 wt.%) within a transparent and amorphous PS matrix as a function of the exposure to different VOCs and the results are discussed in terms of sensitivity and reproducibility of the fluorescence response of the systems. Different julolidine FMRs were utilized, i.e. DCVJ, 9-(2-carboxy-2-cyanovinyl)julolidine (CCVJ) and 9-(2-(1H,1H,2H,2H-perfluorodecyloxycarbonyl)-2-cyanovinyl)julolidine (F8CVJ), in order to identify best suited molecular rotors for sensor performance. The perfluorodecyl chain was selected to favour fluorophore segregation near the film–air interface as to be more responsive to VOC exposure.

2. Experimental part

2.1. Materials and methods

Julolidine, *N,N'*-dicyclohexylcarbodiimide (DCC), phosphorous oxychloride, 9-(2,2-dicyanovinyl)julolidine, 9-(2-carboxy-2-cyanovinyl)julolidine were purchased from Aldrich and used as received. Cyanoacetic acid (Aldrich) was recrystallized from a mixture of toluene/acetone 2:3 v/v. *N,N*-dimethylformamide and dichloromethane (Aldrich) were refluxed over CaH₂ for 2 h and distilled under nitrogen. Tetrahydrofuran (Aldrich) was refluxed over Na/K alloy for 3 h and distilled under nitrogen. Triethylamine (Aldrich) was refluxed over KOH for 3 h and distilled under nitrogen. 1H,1H,2H,2H-perfluorodecyl alcohol (Fluorochem) was used as received. Atactic polystyrene (PS, Repsol, *M_w* = 86,000 g/mol) was used as received. Spectroscopy grade solvents (Carlo Erba or Aldrich) were utilized without further purification.

2.2. Synthesis of 9-formyljulolidine (1)

The synthesis of 9-formyljulolidine (1) was carried out modifying a reported procedure [33]. In brief, phosphorous oxychloride (0.29 mL, 3.17 mmol) was added dropwise to a solution of julolidine (0.5 g, 2.88 mmol) and *N,N*-dimethylformamide (0.27 mL, 3.45 mmol) in anhydrous dichloromethane (5 mL) and the mixture was stirred for 8 h at 25 °C. The reaction was treated with an

aqueous solution of sodium hydroxide (2 M) and the mixture was stirred at 0 °C for 4 h. The organic layer was extracted with diethyl ether, dried over Na₂SO₄ and evaporated to dryness under reduced pressure. The crude product was purified by column chromatography on silica gel (230–400 mesh) using diethyl ether/*n*-hexane (3/7 v/v) as eluent mixture (*R_f* = 0.37) (60% yield).

FT-IR (KBr, cm⁻¹): 2950, 2895, 1662, 1600, 1320, 900, 720.

¹H NMR (CDCl₃) (ppm): 9.6 (s, 1H, CHO), 7.3 (s, 2H, aromatic), 3.3 (t, 4H NCH₂), 2.7 (t, 4H NCH₂CH₂CH₂), 1.9 (m, 4H NCH₂CH₂).

¹³C NMR (CDCl₃) (ppm): 191.3 (CHO), 149.1 (=C–N aromatic), 128.5 to 122.0 (aromatic), 49.3 (NCH₂), 28.1 to 20.4 (NCH₂CH₂CH₂).

EI-MS *m/z* (%): 201 (100, M⁺).

The spectral properties of this compound are in agreement with those previously reported [33].

2.3. Synthesis of 1H,1H,2H,2H-perfluorodecyl cyanoacetate (2)

A solution of 1.03 g (5 mmol) of DCC in 5 mL of anhydrous dichloromethane was added dropwise to a solution of cyanoacetic acid (0.43 g, 5 mmol) and 1H,1H,2H,2H-perfluorodecyl alcohol (2.32 g, 5 mmol) in anhydrous dichloromethane (10 mL). The mixture was kept under stirring for 24 h at 25 °C. Then, it was diluted with dichloromethane (10 mL) and the precipitate formed during the reaction was filtered off. The filtrate was dried under vacuum and the residue was purified by column chromatography on silica gel (230–400 mesh) using dichloromethane as eluent (*R_f* = 0.91) (41% yield).

FT-IR (KBr, cm⁻¹): 2980, 2960, 2188, 1756, 1355–1055, 660.

¹H NMR (CDCl₃) (ppm): 4.6 (t, 2H, CH₂CH₂CF₂), 3.5 (s, 2H, CNCH₂COO), 2.6 (m, 2H CH₂CF₂).

¹³C NMR (CDCl₃) (ppm): 164.2 (COO), 114.6 (CN), 123 to 107 (CF), 56.3 (OCH₂), 31.8 (OCH₂CH₂), 26.0 (CH₂CN).

Anal. Calcd for C₁₃H₆F₁₇NO₂: C, 29.40; H, 1.14. Found: C, 30.0; H, 1.0.

2.4. Synthesis of 9-(2-(1H,1H,2H,2H-perfluorodecyloxycarbonyl)-2-cyanovinyl)julolidine (F8CVJ)

Triethylamine (0.3 mL, 2.14 mmol) was added to a solution of 2 (0.83 g, 1.56 mmol) and 1 (0.21 g, 1.06 mmol) in tetrahydrofuran (8 mL) and the mixture was stirred at 50 °C for 10 h. The solvent was then evaporated and the residue was purified in a first step by column chromatography on silica gel using dichloromethane/*n*-hexane (4/6 v/v) as mobile phase. The obtained product was further purified by elution on preparative TLC plates using ethyl acetate/*n*-hexane (4/6 v/v) as eluent mixture (*R_f* = 0.59) (20% yield).

FT-IR (KBr, cm⁻¹): 2925, 2855, 2215, 1720, 1615–1525, 1450, 1322–1130, 660.

¹H NMR (CDCl₃) (ppm): 7.9 (s, 1H, CNCCH), 7.5 (s, 2H, aromatic), 4.5 (t, 2H, COOCH₂), 3.3 (t, 4H, NCH₂), 2.7 (t, 4H, NCH₂CH₂CH₂), 2.6 (m, 4H, CH₂CF₂), 1.9 (m, 4H, NCH₂CH₂).

¹³C NMR (CDCl₃) (ppm): 164.4 (COO), 154.8 (PhCH =), 147.8 (=C–N aromatic), 128.2 to 121.0 (aromatic), 117.6 (CN), 123–107 (CF), 57.3 (OCH₂), 50.2 (NCH₂), 27.2–21.0 (NCH₂CH₂CH₂).

¹⁹F NMR (CDCl₃/CF₃COOH) (ppm): –6 (CF₃), –38 (2F, CH₂CF₂), –49 to –47 (10F, CF₂), –52 (2F, CF₂CF₃).

EI-MS *m/z* (%): 95 (48), 186 (15), 251 (15), 267 (16), 463 (8).

2.5. Preparation of polymeric films

Films of julolidine derivative/PS mixtures were prepared by dissolving 1 g of PS and the desired amount of dye (0.005–0.1 wt.%) in 150 mL of CHCl₃. After solvent evaporation, the polymer mixture was melt-pressed between two Teflon foils in a Carver 3851-0 press at 150 °C and 4 tons of pressure for 5 min. After removal from the

press, the films (180–220 μm thick) were allowed to reach slowly room temperature.

2.6. Characterization

^1H NMR and ^{19}F NMR spectra were recorded with a Varian Gemini VRX300 spectrometer on CDCl_3 or $\text{CDCl}_3/\text{CF}_3\text{COOH}$ solutions, respectively, whereas ^{13}C NMR spectra were accomplished with a Varian Gemini 600 spectrometer on CDCl_3 solutions. EI-MS spectra were measured at 70 eV by GLC/MS. Infrared spectra were recorded by a Fourier transform infrared spectrometer (Spectrum One, PerkinElmer) on KBr windows. UV–Vis spectra of THF solutions were recorded at room temperature in isotropic conditions with a Perkin Elmer Lambda 650.

Fluorescence spectra of solutions were recorded ($\lambda_{\text{exc.}} = 450 \text{ nm}$) at room temperature with a Horiba Jobin-Yvon Fluorolog[®]-3 spectrofluorometer. The fluorescence quantum yield (Φ_f) in ethanol was determined at room temperature relative to fluorescein ($\Phi_f^s = 0.79$ in 0.1 N NaOH) using Equation (1):

$$\Phi_x = \Phi_{\text{ST}} \left(\frac{\text{Grad}_x}{\text{Grad}_{\text{ST}}} \right) \left(\frac{n_{\text{ST}}^2}{n_x^2} \right) \quad (1)$$

where the subscripts ST and X are standard and dye respectively, Grad the gradient from the plot of integrated fluorescence intensity vs absorbance for different solutions of standard and dyes. In order to minimize re-absorption effects, absorbances never exceeded 0.1 in correspondence and above the excitation wavelength. n is the refractive index of the solvent, i.e. 1.3611 for ethanol, 1.4746 for glycerol and 1.333 for water.

The viscosity of EtOH/glycerol mixtures was predicted with good approximation by a simple additive rule: [39]

$$\log \eta = \sum_{i=1}^2 \phi_i \log \eta_i \quad (2)$$

where η is the viscosity of solvent mixture, ϕ_i and η_i are the volume fraction and viscosity of the component i , respectively.

Fluorescence spectra of polymer films were recorded ($\lambda_{\text{exc.}} = 450 \text{ nm}$) in the dark by using the F-3000 Fiber Optic Mount apparatus coupled with optical fibre bundles. Light is focused from the excitation spectrometer into the optical fibre bundles, and then directed to the sample. Fluorescence emission from the sample is directed back through the bundle and into the front-face collection port in the sample compartment.

The fluorescence variation of the films was tested by exposing the film at room temperature to VOCs, such as hexane, heptane, toluene, chloroform, tetrahydrofuran, acetone, dioxane and methanol. The film was attached to an aluminium foil, which covers a closed container as shown in Fig. 1.

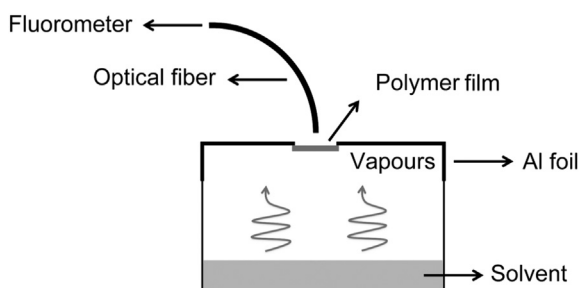


Fig. 1. Schematic apparatus used to study the vapour sensing behavior.

Solvent uptake by polymer films was determined by placing the aluminium foil/polymer film system in a Gibertini E 50 S/2 analytical balance with five significant figures.

Thermogravimetric scans were carried out by a Mettler Toledo Starc System (TGA/SDTA851[®]). Samples were heated from 25 to 800 °C at 10 °C/min under a nitrogen flow.

Film thickness was measured with a Starrett[®] V230MXFL outside micrometer having an accuracy of $\pm 0.002 \text{ mm}$.

Angle-resolved X-ray photoelectron spectroscopy (XPS) spectra were recorded by using a Perkin–Elmer PHI 560 spectrometer with a standard Al-K α source (1486.6 eV) operating at 350 W. The working pressure was less than 10^{-8} Pa . The spectrometer was calibrated by assuming the binding energy (BE) of the Au 4f_{7/2} line to be 84.0 eV with respect to the Fermi level. Extended (survey) spectra were collected in the range of 0–1350 eV (187.85 eV pass energy, 0.4 eV step, 0.05 s/step). The spectra were recorded at the two photoemission angles θ (between the path taken by the photoelectrons to the detector and the surface normal) of 70° and 20°. The standard deviation (SD) in the BE values of the XPS line was 0.10 eV. The atomic percentage, after a Shirley type background subtraction [40], was evaluated using the PHI sensitivity factors. To take into account charging problems, the C(1s) peak was considered at 285.0 eV and the peak BE differences were evaluated. The effective information depth varies according to $d = d_0 \cos \theta$, where d_0 is the maximum information depth ($d_0 \sim 10 \text{ nm}$ for the C(1s) line with an Al-K α source).

3. Results and discussion

DCVJ and CCVJ are commercially available, whereas novel F8CVJ was synthesized from julolidine (Fig. 2).

In detail, commercially available julolidine was formylated with phosphorus oxychloride and dimethylformamide to afford 9-formyljulolidine. The fluorinated cyanoacetic ester was obtained via dicyclohexyl carbodiimide-induced esterification of cyanoacetic acid with 1*H*,1*H*,2*H*,2*H*-perfluorodecyl alcohol. Condensation of the ester with 9-formyljulolidine in the presence of triethylamine produced the desired F8CVJ.

3.1. Spectroscopic characterization of DCVJ, CCVJ and F8CVJ solutions

Absorption and emission maxima of DCVJ, CCVJ and F8CVJ in ethanol solutions were all in the blue-green range, with emission maxima between 470 and 500 nm. Quantum yields were negligible (Table 1), due to the formation of a TICT excited state, which rapidly decayed in a non-radiative way through internal rotation [23,25].

The higher quantum yield of F8CVJ with respect those of DCVJ and CCVJ was attributed to a more restricted intramolecular twisting motion which favours the emission of light from the LE state of the dye [23,25].

All compounds exhibited a noteworthy viscosity-dependent fluorescence emission when glycerol was added to ethanol solutions (Fig. 3 and Table 2).

All FMRs experienced a strong increase in quantum yield (about 10–20 times higher) when dissolved in viscous environments like glycerol solutions (viscosity $\eta = 945 \text{ mPa s}$ at 20 °C for glycerol, as compared to 1.2 mPa s for EtOH). According to the literature [27], in viscous media the molecular internal rotation is hindered, thus favouring a radiative decay of the LE state and an increase in quantum yield. Conversely, the emission wavelength appeared less sensitive to polarity variations (dielectric constant $\epsilon = 45.2$ for glycerol, as compared to 25 for EtOH) and only a red-shift by about 10 nm occurred for all compounds. DCVJ, CCVJ and F8CVJ FMRs can

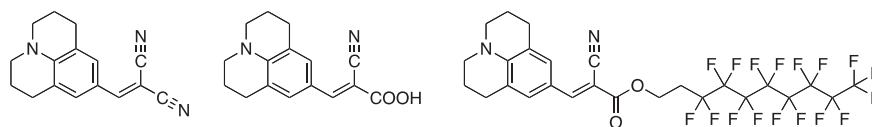


Fig. 2. 9-Dicyanovinyljulolidine (DCVJ, left), 9-(2-carboxy-2-cyanovinyl)julolidine (CCVJ, middle) and 9-(2-(1H,1H,2H,2H-perfluorodecyloxycarbonyl)-2-cyanovinyl)julolidine (F8CVJ, right).

be therefore utilized as viscosity probes even in environments where polarity changes are expected.

All the FMRs followed a Förster-Hoffmann behaviour according to Equation (3) (Fig. S1, Supplementary information), which relates the (double logarithmic) correlation of quantum yield with viscosity:

$$\log \Phi_f = C + x \cdot \log \eta \quad (3)$$

where C and x are constants. η was calculated by using Equation (2) (see Experimental part).

In all cases, the x parameter, i.e. the viscosity sensitivity of the FMR, was found to be between 0.36 and 0.57, in agreement with the values reported in literature [41]. Interestingly, F8CVJ, which showed the highest fluorescence emission in EtOH, appeared as the FMR with the lowest viscosity sensitivity. This suggests that in solution less emission intensity at low viscosity regime would help the FMR be more sensitive to viscosity variation than a brighter dye.

3.2. Spectroscopic characterization of FMR/polystyrene films

DCVJ, CCVJ and F8CVJ FMRs were dispersed in polystyrene (PS) at different concentration in the range between 0.005 and 0.1 wt.%. All the films appeared well homogeneous, optically transparent with absorption features similar to those collected in solution. The concentration of 0.05 wt.% was then selected for all FMRs in order to provide PS films with appropriate luminescent responses without encountering possible quenching phenomena due to concentration.

PS is an amorphous polymer with a glass transition temperature of about 90–100 °C and negligible absorption and emission features in the wavelength range investigated (Fig. S2). Thus, the dyes were dispersed in a glassy matrix in which the intramolecular rotations of their julolidine fluorophores were in fact completely arrested. This would favour the emission of light from their LE states. Recently, Iasilli et al. found that when tetraphenylethylene (TPE) FMR was dispersed in a glassy PS matrix, the arrested intramolecular rotations of its aryls resulted in a strong emission of light, whereas fluorescence significantly weakened when viscous but not glassy polymer matrices were used [42].

Consistent with those findings, the fluorescence spectra of DCVJ/PS, CCVJ/PS and F8CVJ/PS films (Fig. 4) showed about 10 nm blue-shifted emission intensities similar to those collected from EtOH/glycerol 10:90 v/v solutions.

This blue shift is ascribed to the lower dielectric constant of the polymer matrix ($\epsilon = 2.6$) as compared to that of solvent mixtures.

Table 1
Optical features of 10^{-5} M DCVJ, CCVJ and F8CVJ ethanol solutions.

| Compound | Absorption max (nm) | Emission max (nm) | Φ_f^a |
|----------|---------------------|-------------------|---------------------|
| DCVJ | 458 | 496 | $1.2 \cdot 10^{-3}$ |
| CCVJ | 444 | 474 | $1.5 \cdot 10^{-3}$ |
| F8CVJ | 448 | 488 | $3.8 \cdot 10^{-3}$ |

^a Fluorescence quantum yield (Φ_f) determined at room temperature relative to fluorescein ($\Phi_f^s = 0.79$ in 0.1 N NaOH), $\lambda_{exc.} = 450$ nm.

The slight difference in emission spectral shape can be possibly attributed to the different dye–polymer interactions caused by the diverse nature of the FMR functional groups [43].

The nature of the functional julolidine moieties also affected the intensity of the emitted light of FMR/PS films. The higher emission intensity of CCVJ/PS with respect to DCVJ/PS reflected the behaviour in solution, i.e. $\Phi_{CCVJ} = 6.0 \cdot 10^{-2}$ and $\Phi_{DCVJ} = 4.2 \cdot 10^{-2}$ (see Table 2), whereas the strong luminescence of F8CVJ/PS film must be due to some peculiar feature of the perfluorodecyl chain. It has been recognized that perfluorinated alkyl chains can be used to impose phase-segregating power onto a given molecule and

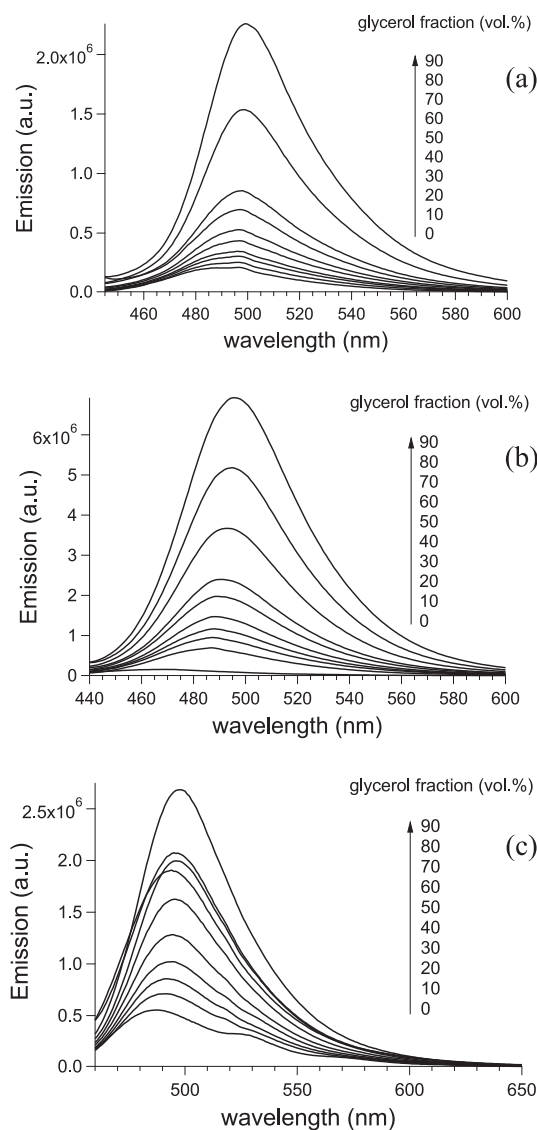


Fig. 3. Fluorescence spectra of (a) DCVJ, (b) CCVJ and (c) F8CVJ dilute solutions ($5 \cdot 10^{-6}$ M) in EtOH/glycerol mixtures with different glycerol volume contents.

Table 2
Optical features of $5 \cdot 10^{-6}$ M DCVJ, CCVJ and F8CVJ EtOH/glycerol 10:90 v/v solutions.

| Compound | Absorption max (nm) | Emission max (nm) | ϕ_f^a |
|----------|---------------------|-------------------|---------------------|
| DCVJ | 469 | 506 | $4.2 \cdot 10^{-2}$ |
| CCVJ | 452 | 484 | $6.0 \cdot 10^{-2}$ |
| F8CVJ | 457 | 497 | $3.3 \cdot 10^{-2}$ |

^a Fluorescence quantum yield (ϕ_f) was determined at room temperature relative to fluorescein. $\lambda_{\text{exc}} = 450$ nm.

fluorinated materials can be used as surface-active components of polymer mixtures [44,45]. Analogously, the perfluorodecyl chain could force F8CVJ molecules to segregate from PS, thus favouring their effective migration to the surface of the polymer films [46,47].

In order to investigate the effects of perfluorodecyl chain on the surface migration and enrichment of dispersed F8CVJ, F8CVJ/PS films were analyzed by angle-resolved X-ray photoelectron spectroscopy (AR-XPS). Spectra were recorded at different photoemission angles, $\theta = 70^\circ$ and 20° , corresponding to increasing probing depths in the range 3–10 nm of the outermost surface. The experimental intensities of C(1s) and F(1s) signals (at binding energies of ~ 290 eV and ~ 690 eV, respectively) were used to evaluate C and F atomic abundances. The C/F ratio at both $\theta = 70^\circ$ (~ 30) and $\theta = 20^\circ$ (~ 15) was much lower than the theoretical one (~ 2500), calculated on the basis of the known stoichiometric composition of the F8CVJ/PS film. Thus, F8CVJ was preferentially concentrated in a ~ 10 nm outer layer of the film surface, owing to the selective segregation of the low surface energy fluorinated fluorophore at the polymer–air interface.

An AR-XPS analysis was also carried out on DCVJ/PS film. The film surface was found to contain only carbon, whereas neither oxygen nor nitrogen could be recorded, being below the detection limit of XPS sensitivity. DCVJ did not migrate to the near-surface region of the polymer film but was buried in the bulk of the PS matrix.

3.3. Effect of vapour exposure on the fluorescence emission of FMR/PS films

One of the peculiarities of FMRs is their fluorescence variation in response to changes in viscosity or sterical constraints. Those effects can also be provided by variations in the free volume of the matrix in which they are dispersed. In fact, the interactions between a polymer and vapours of a suitable solvent are able to induce a relaxation of macromolecular chains which is followed by a greater mobility with an increase in the free volume and a consequent decrease in the local microviscosity [48]. It is therefore expected that the fluorescence emission of an FMR embedded in a polymer matrix could be affected by vapour exposure. We explored

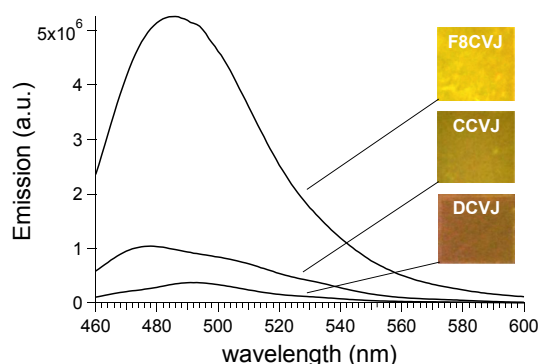


Fig. 4. Emission spectra of 0.05 wt.% DCVJ/PS, CCVJ/PS and F9CVJ/PS films and (inset) images of the films taken under the illumination at 450 nm.

the effect of several VOCs on the fluorescence properties of FMR/PS films, by selecting different kinds of organic solvents.

An illustration of the fluorescence emission dependence on exposure time to chloroform vapours is shown in Fig. 5. Notably, the 0.05 wt.% DCVJ/PS films underwent a significant variation in emission intensity when exposed to a saturated atmosphere of chloroform (Fig. 5).

The emission intensity dropped by about 50% just after 420 s of exposure. This solvent dependence was ascribed to the FMR sensitivity of the DCVJ molecule and resides in the reorganization energy of the excited transition state (from LE to TICT states) with increasing solvent uptake. PS matrix is in the glassy state with an associated large fraction of free volume in the form of channels and holes of molecular dimensions. When chloroform vapours fill these empty spaces, diffusion and swelling of the polymer start from the outer surface layers inwards. As a consequence, the swollen layers contain the polymer material in a viscous state, thus making the intramolecular rotations of julolidine moieties to occur more freely [27]. This phenomenon resulted in a decreased emission intensity of DCVJ. The concomitant shift to longer wavelengths, i.e. from 480 to about 500 nm, was possibly due to the higher dielectric constant of chloroform with respect to PS ($\epsilon_{\text{chloroform}} = 4.81$ and $\epsilon_{\text{PS}} = 2.6$).

CCVJ/PS and F8CVJ/PS films exhibited a quite different behaviour upon exposure to chloroform vapours (Fig. 6). The fluorescence variation appeared more pronounced and reached a plateau after about 350–400 s for both films, in contrast to DCVJ/PS films, which displayed a lesser reduction in fluorescence emission without levelling off to a constant value. The fastest response observed for F8CVJ/PS films, whose emission amplitude decreased by 50% just after 100 s of exposure, suggests that a larger variation in luminance would result for FMRs that are more sterically constrained and carry functional groups that adversely affect their phase dispersion within PS. The carboxylic unit in CCVJ and, more evidently, the perfluorodecyl chain in F8CVJ enable the julolidine FMR to interact more readily with chloroform. Such interaction was facilitated for the latter FMR that was distributed closely to the film surface.

The curves actually reflected the weight of chloroform progressively adsorbed by time by PS films (Fig. S3). After 420 s, the system reached an equilibrium since the film across its whole thickness was involved in solvent permeation. All FMR molecules were embedded in a polymer environment with homogeneous microviscosity and their emission did not change any longer for prolonged exposure times.

The fluorescence variation of FMR/PS films appeared similar when toluene was utilized as a probing VOC (Fig. 7). However, the amplitude decrease of the emission reduced in extent and was significantly slower, by about 6 times, than that shown with

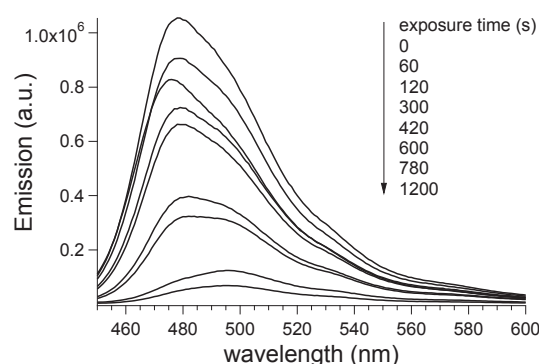


Fig. 5. Progressive changes in the fluorescence emission of 0.05 wt.% DCVJ/PS film as a function of the exposure to chloroform vapours.

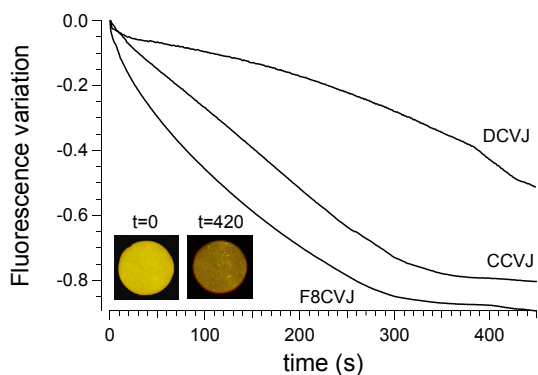


Fig. 6. Variation of the fluorescence maximum intensity with exposure time for all 0.05 wt.% FMR/PS films with inset images of the 0.05 wt.% F8CVJ/PS film before ($t = 0$ s) and after ($t = 420$ s) chloroform exposure.

chloroform. This behaviour can be attributed to the lower vapour pressure of toluene (i.e., 2.9 kPa for toluene against 21.3 kPa for chloroform, at 25 °C) [49], which can delay solvent adsorption by the film during the initial stages of exposure. However, the fluorescence emission did not experience any variation in amplitude when methanol was used as a VOC (Fig. 7).

This behaviour can arise from a combination of effects: the lower vapour pressure of methanol (i.e., 12.7 kPa for methanol against 21.3 kPa for chloroform, at 25 °C) [49], which can delay solvent adsorption by the film, and the limited affinity between methanol and PS. This feeble interaction hampers methanol uptake by the polymer, thus making the fluorescence variation of the films negligible. This is in agreement with the more unfavourable Flory–Huggins interaction parameter (χ) of 2.44 for methanol [50] compared to 0.52–0.17 for chloroform [51] and 0.42–0.31 for toluene [51] at 25 °C. Moreover, PS films appeared responsive also to tetrahydrofuran ($\chi = 0.16$ –0.70), acetone ($\chi = 0.81$ –0.94) and dioxane ($\chi = 0.35$, Fig. S4), whereas the emission was barely affected by hexane, cyclohexane and heptane ($\chi = 1.49$ –1.14) vapours. These results suggest that the selectivity of FMR/PS films is determined by the chemical affinity of PS for the solvent vapours. More specifically, solvents with χ values lower than 1–2 well interact with the PS matrix, thus providing the vapour sensing behaviour.

The PS films based on CCVJ and F8CVJ, i.e. those FMRs characterized by the largest vapour response, were then exposed to chloroform/methanol mixtures in order to determine whether the system could be sensitive and selective to mixed vapours of varied

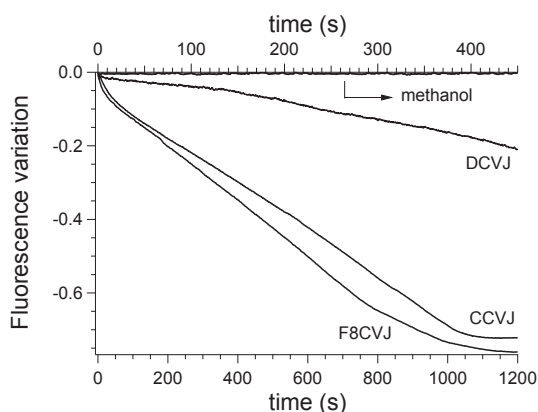


Fig. 7. Variation of the fluorescence maximum with exposure time to toluene and methanol (superimposed curves with no variation) vapours for 0.05 wt.% FMR/PS films.

composition (Fig. 8). Methanol was actually utilized as a sort of diluent for chloroform.

Comparing the fluorescence variations recorded by exposing the CCVJ/PS (Fig. 8a) and F8CVJ/PS (Fig. 8b) films to solvent mixtures of different vol.% of chloroform, the fluorescence variation became progressively smaller in extent, according to the decreasing amount of chloroform in the vapour composition. Moreover, the curves recorded with solutions rich in methanol showed a continuous descending response without levelling off, thereby suggesting incompleteness of the phenomenon within the collection time of 450 s.

Notably, the F8CVJ/PS films appeared more sensitive to solvent vapours than CCVJ/PS films, with the fluorescence emission being responsive even to 25 vol.% chloroform in the solution. This result was in agreement with the F8CVJ characteristics, being the perfluorodecyl chain properly designed to provide the julolidine FMR with a highest sensitivity to VOCs, thanks to its favourable distribution close to the PS film surface. The PS/F8CVJ films sensitivity limit of 25 vol.% chloroform in the solution corresponds to about 45–50 vol.% in the vapour phase. [52]

The experimental setup consists in vapour exposure at ambient temperature and pressure, and it did not affect sample size or morphology within the time interval investigated (<20 min). Solvent then gradually desorbed at room temperature and pressure from the film when removed from the apparatus, allowing complete recovery of the FMR emission after 24 h. This behaviour suggested to monitor changes in FMR/PS fluorescence during successive solvent exposures. Fig. 9 illustrates the response of F8CVJ/PS films to a sequence of solvent adsorption and subsequent slow desorption at room temperature and pressure for 24 h.

Notably, the fluorescence variation of the samples was well retained also after repeated cycles of solvent adsorption/desorption, thereby indicating a very good reproducibility in the optical response. All results were confirmed when desorption steps were carried out at 50 °C for 1 h (data not shown). Similar trends were also collected by using toluene as VOC, even if slightly lower reproducibility of the fluorescence variation was observed during initial solvent uptake. Whilst toluene may have a larger influence

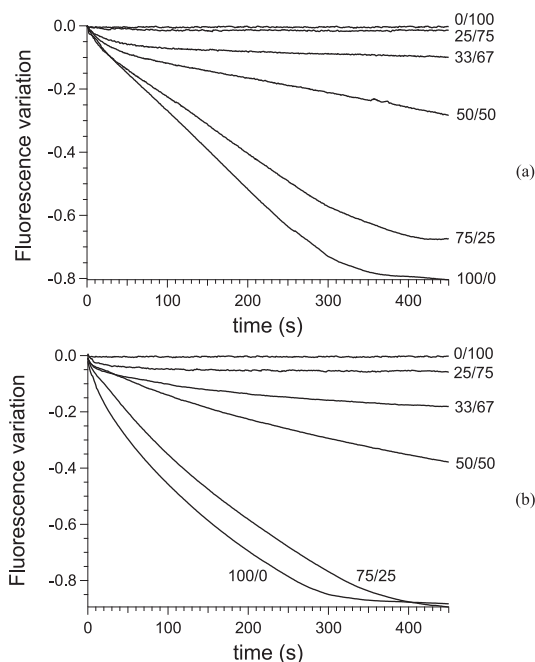


Fig. 8. Variation of the fluorescence maximum with exposure time to vapours of chloroform/methanol mixtures (v/v) for 0.05 wt.% (a) CCVJ/PS and (b) F8CVJ/PS films.

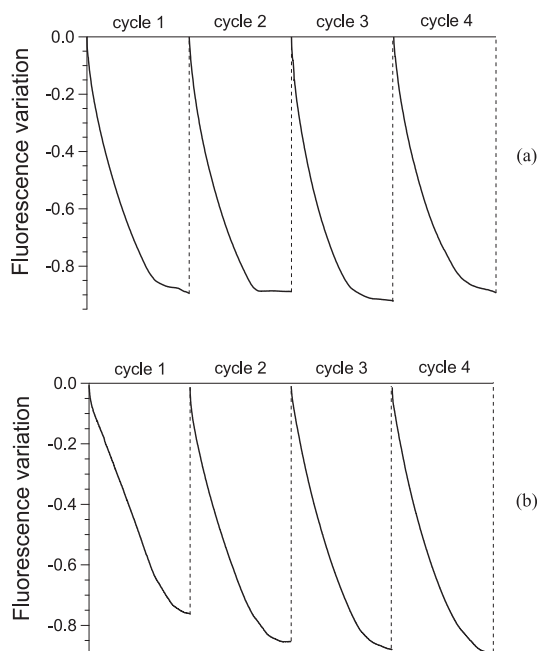


Fig. 9. Variation of the fluorescence maximum of F8CVJ/PS films for successive cycles of solvent exposure/desorption to (a) chloroform and (b) toluene vapours.

on the PS film morphology during the first cycle of solvent adsorption/desorption, F8CVJ appeared to experience no substantial modification of its distribution within PS film across the whole experiments.

4. Conclusions

We have shown that julolidine FMRs can be utilized as effective dyes for the preparation of plastic films with vapour sensing characteristics.

FMRs exhibited viscosity-dependent emission properties when dissolved in solvents with different viscosity or dispersed at low loadings (<0.1 wt.%) in PS plastic films. The exposure of FMR/PS films to a saturated atmosphere of well-interacting VOCs caused a significant drop of FMR fluorescence due to their favoured relaxation from the non-emissive TICT excited state. This optical behaviour was allowed by the increased mobility of the PS macromolecular chains with solvent uptake, and was largely enhanced for the F8CVJ FMR that was preferentially distributed at the outer film surface. By contrast, the film emission appeared unaffected when methanol and hexane were used as solvents barely interacting with PS. This characteristic response made plastic films able to discern vapours of different composition, providing also a sensitive and reproducible fluorescence response in successive cycles of solvent exposure. FMR/PS films might be exploited for the realization of reliable vapour sensing plastic materials as new tools to detect vapours of different classes of VOCs.

Acknowledgements

This work was supported by MIUR-PRIN (2010XLLNM3). The authors are grateful to Dr. A. Glisenti (University of Padova) for assistance with XPS measurements.

Appendix A. Supplementary data

Supplementary data related to this article can be found at <http://dx.doi.org/10.1016/j.dyepig.2014.07.025>.

References

- [1] Hagfeldt A, Boschloo G, Sun L, Kloo L, Pettersson H. Dye-sensitized solar cells. *Chem Rev* 2010;110(11):6595–663.
- [2] He GS, Tan L-S, Zheng Q, Prasad PN. Multiphoton absorbing materials: molecular designs, characterizations, and applications. *Chem Rev* 2008;108(4):1245–330.
- [3] Prampolini G, Bellina F, Biczysko M, Cappelli C, Carta L, Lessi M, et al. Computational design, synthesis, and mechanochromic properties of new thiophene-based p-conjugated chromophores. *Chem Eur J* 2013;19(6):1996–2004.
- [4] Ciardelli F, Ruggeri G, Pucci A. Dye-containing polymers: methods for preparation of mechanochromic materials. *Chem Soc Rev* 2013;42(3):857–70.
- [5] Pucci A, Ruggeri G, Bronco S, Bertoldo M, Cappelli C, Ciardelli F. Conferring dichroic properties and optical responsiveness to polyolefins through organic chromophores and metal nanoparticles. *Progr Org Coat* 2007;58(2–3):105–16.
- [6] Minei P, Battisti A, Barondi S, Lessi M, Bellina F, Ruggeri G, et al. Light-responsive polystyrene films doped with tailored heteroaromatic-based fluorophores. *ACS Macro Lett* 2013;2(4):317–21.
- [7] Ciardelli F, Bertoldo M, Bronco S, Pucci A, Ruggeri G, Signori F. The unique optical behaviour of bio-related materials with organic chromophores. *Polym Int* 2013;62(1):22–32.
- [8] Makowski B, Kunzelman J, Weder C. Stimuli-driven assembly of chromogenic dye molecules: a versatile approach for the design of responsive polymers. In: Urban MW, editor. *Handbook of stimuli-responsive materials*. Weinheim, Germany: Wiley-VCH Verlag GmbH & Co. KGaA; 2011. p. 117–38.
- [9] Wenger OS. Vapochromism in organometallic and coordination complexes: chemical sensors for volatile organic compounds. *Chem Rev* 2013;113(5):3686–733.
- [10] Hong Y, Lam JWY, Tang BZ. Aggregation-induced emission: phenomenon, mechanism and applications. *Chem Commun* 2009;29:4332–53.
- [11] Chi Z, Zhang X, Xu B, Zhou X, Ma C, Zhang Y, et al. Recent advances in organic mechanofluorochromic materials. *Chem Soc Rev* 2012;41(10):3878–96.
- [12] Yoon J, Chae SK, Kim J-M. Colorimetric sensors for volatile organic compounds (VOCs) based on conjugated polymer-embedded electrospun fibers. *J Am Chem Soc* 2007;129(11):3038–9.
- [13] Kim S-H, Lee S-Y, Gwon S-Y, Son Y-A, Bae J-S. D- π -A solvatochromic charge transfer dyes containing a 2-cyanomethylene-3-cyano-4,5,5-trimethyl-2,5-dihydrofuran acceptor. *Dyes Pigments* 2010;84(2):169–75.
- [14] Zhang X, Chi Z, Li H, Xu B, Li X, Zhou W, et al. Piezofluorochromism of an aggregation-induced emission compound derived from tetraphenylethylene. *Chem Asian J* 2011;6(3):808–11.
- [15] Zhang X, Chi Z, Li H, Xu B, Li X, Liu S, et al. Synthesis and properties of novel aggregation-induced emission compounds with combined tetraphenylethylene and dicarbazolyl triphenylethylene moieties. *J Mater Chem* 2011;21(6):1788–96.
- [16] Chen Q, Wang J-X, Yang F, Zhou D, Bian N, Zhang X-J, et al. Tetraphenylethylene-based fluorescent porous organic polymers: preparation, gas sorption properties and photoluminescence properties. *J Mater Chem* 2011;21(35):13554–60.
- [17] Shustova NB, McCarthy BD, Dinca M. Turn-On fluorescence in tetraphenylethylene-based metal-organic frameworks: an alternative to aggregation-induced emission. *J Am Chem Soc* 2011;133(50):20126–9.
- [18] Hong Y, Lam JWY, Tang BZ. Aggregation-induced emission. *Chem Soc Rev* 2011;40(11):5361–88.
- [19] Wang J, Mei J, Hu R, Sun JZ, Qin A, Tang BZ. Click synthesis, aggregation-induced emission, E/Z isomerization, self-organization, and multiple chromisms of pure stereoisomers of a tetraphenylethylene-cored luminogen. *J Am Chem Soc* 2012;134(24):9956–66.
- [20] Kumpfer JR, Taylor SD, Connick WB, Rowan SJ. Vapochromic and mechanochromic films from square-planar platinum complexes in polymethacrylates. *J Mater Chem* 2012;22(28):14196–204.
- [21] Lim SH, Feng L, Kemling JW, Musto CJ, Suslick KS. An optoelectronic nose for the detection of toxic gases. *Nat Chem* 2009;1:562–7.
- [22] Haidekker MA, Nipper M, Mustafic A, Lichlyter D, Dakanali M, Theodorakis EA. Dyes with segmental mobility: molecular rotors. *Springer Ser Fluoresc* 2010;8:267–308. *Advanced Fluorescence Reporters in Chemistry and Biology I*.
- [23] Haidekker MA, Theodorakis EA. Molecular rotors-fluorescent biosensors for viscosity and flow. *Org Biomol Chem* 2007;5(11):1669–78.
- [24] Haidekker MA, Theodorakis EA. Environment-sensitive behaviour of fluorescent molecular rotors. *J Biol Eng* 2010;4(11):1–14.
- [25] Zhou F, Shao J, Yang Y, Zhao J, Guo H, Li X, et al. Molecular rotors as fluorescent viscosity sensors: molecular design, polarity sensitivity, dipole moments changes, screening solvents, and deactivation channel of the excited states. *Eur J Org Chem* 2011;2011(25):4773–87. S1–S/70.
- [26] Amdursky N, Erez Y, Huppert D. Molecular rotors: what lies behind the high sensitivity of the thioflavin-T fluorescent marker. *Acc Chem Res* 2012;45(9):1548–57.
- [27] Valeur B, Berberan-Santos MN. *Molecular fluorescence: principles and applications*. Weinheim (Germany): Wiley-VCH; 2012.
- [28] Zhu L-L, Qu D-H, Zhang D, Chen Z-F, Wang Q-C, Tian H. Dual-mode tunable viscosity sensitivity of a rotor-based fluorescent dye. *Tetrahedron* 2010;66(6):1254–60.

- [29] Là Zhu, Li X, Ji F-Y, Ma X, Wang Q-C, Tian H. Photolockable ratiometric viscosity sensitivity of cyclodextrin polypseudorotaxane with light-active rotor graft. *Langmuir* 2009;25(6):3482–6.
- [30] Rumble C, Rich K, He G, Maroncelli M. CCVJ is not a simple rotor probe. *J Phys Chem A* 2012;116(44):10786–92.
- [31] Nipper ME, Majd S, Mayer M, Lee JCM, Theodorakis EA, Haidekker MA. Characterization of changes in the viscosity of lipid membranes with the molecular rotor FCVJ. *Biochim Biophys Acta Biomembr* 2008;1778(4):1148–53.
- [32] Goh WL, Lee MY, Joseph TL, Quah ST, Brown CJ, Verma C, et al. Molecular rotors as conditionally fluorescent labels for rapid detection of biomolecular interactions. *J Am Chem Soc* 2014;136(17):6159–62.
- [33] Haidekker MA, Ling T, Anglo M, Stevens HY, Frangos JA, Theodorakis EA. New fluorescent probes for the measurement of cell membrane viscosity. *Chem Biol* 2001;8(2):123–31.
- [34] Maity D, Manna AK, Karthigeyan D, Kundu TK, Pati SK, Govindaraju T. Visible-near-infrared and fluorescent copper sensors based on julolidine conjugates: selective detection and fluorescence imaging in living cells. *Chem Eur J* 2011;17(40):11152–61. S/1–S/40.
- [35] Haidekker MA, Akers W, Lichlyter D, Brady TP, Theodorakis EA. Sensing of flow and shear stress using fluorescent molecular rotors. *Sens Lett* 2005;3(1–1):42–8.
- [36] Zhu D, Haidekker MA, Lee J-S, Won Y-Y, Lee JCM. Application of molecular rotors to the determination of the molecular weight dependence of viscosity in polymer melts. *Macromolecules* 2007;40(21):7730–2.
- [37] Jee A-Y, Bae E-H, Lee M-Y. Internal twisting dynamics of dicyanovinyljulolidine in polymers. *J Phys Chem B* 2009;113(52):16508–12.
- [38] Xiao P, Frigoli M, Dumur F, Graff B, Gignes D, Fouassier JP, et al. Julolidine or fluorenone based push-pull dyes for polymerization upon soft polychromatic visible light or green light. *Macromolecules* 2014;47(1):106–12.
- [39] Perry RH, Green DW, Maloney JO. Perry's chemical engineer's handbook. 6th ed. New York: McGraw-Hill; 1984.
- [40] Shirley DA. High-resolution X-ray photoemission spectrum of the valence bands of gold. *Phys Rev B* 1972;5(12):4709–14.
- [41] Sutharsan J, Lichlyter D, Wright NE, Dakanali M, Haidekker MA, Theodorakis EA. Molecular rotors: synthesis and evaluation as viscosity sensors. *Tetrahedron* 2010;66(14):2582–8.
- [42] Iasilli G, Battisti A, Tantussi F, Fuso F, Allegrini M, Ruggeri G, et al. Aggregation-induced emission of tetraphenylethylene in styrene-based polymers. *Macromol Chem Phys* 2014;215:499–506.
- [43] Pucci A, Tirelli N, Ruggeri G, Ciardelli F. Absorption and emission dichroism of polyethylene films with molecularly dispersed push-pull terthiophenes. *Macromol Chem Phys* 2005;206(1):102–11.
- [44] Galli G, Martinelli E, Chiellini E, Ober CK, Glisenti A. Low surface energy characteristics of mesophase-forming ABC and ACB triblock copolymers with fluorinated B blocks. *Mol Cryst Liq Cryst* 2005;441(1):211–26.
- [45] Yasani BR, Martinelli E, Galli G, Glisenti A, Mieszkin S, Callow ME, et al. A comparison between different fouling-release elastomer coatings containing surface-active polymers. *Biofouling* 2014;30(4):387–99.
- [46] Hunley MT, Harber A, Orlicki JA, Rawlett AM, Long TE. Effect of hyperbranched surface-migrating additives on the electrospinning behavior of poly(methyl methacrylate). *Langmuir* 2007;24(3):654–7.
- [47] Martinelli E, Fantoni C, Galli G, Gallot B, Glisenti A. Low surface energy properties of smectic fluorinated block copolymer/SEBS blends. *Mol Cryst Liq Cryst* 2009;500(1):51–62.
- [48] Miller-Chou BA, Koenig JL. A review of polymer dissolution. *Prog Polym Sci* 2003;28(8):1223–70.
- [49] Lide DR. CRC handbook of chemistry and physics. 86th ed. Boca Raton, FL, USA: CRC Press LLC; 2004.
- [50] Bernardo G, Vesely D. Equilibrium solubility of alcohols in polystyrene attained by controlled diffusion. *Eur Polym J* 2007;43(3):938–48.
- [51] Mark JE. Physical properties of polymers handbook. 2nd ed. New York: Springer Science + Business Media, LLC; 2007.
- [52] Martin M, Cocero M, Mato F. Vapor-liquid equilibrium data at 25 °C for six binary systems containing methyl acetate or methanol, with dichloromethane, chloroform, or 1,2-trans-dichloroethylene. *J Solut Chem* 1991;20(1):87–95.